Theoretical Determination of Two Structural Forms of the Active Site in Cadmium-Containing Phosphotriesterases

Fang Zheng,[†] Chang-Guo Zhan,*[,‡] and Rick L. Ornstein[†]

Department of Medicine, College of Physicians & Surgeons, Columbia University, New York, New York 10032, and Pacific Northwest National Laboratory, Mailstop K1-83, Battelle Boulevard, P.O. Box 999, Richland, Washington 99352

Received: August 7, 2001; In Final Form: October 15, 2001

Two structural forms of the active site in Cd^{2+}-containing phosphotriesterases (PTE), i.e., Cd^{2+}/Cd^{2+}−PTE and Zn^{2+}/Cd^{2+}−PTE, were determined by performing ab initio and density functional theory calculations on active site models. The calculated results indicate that the second bridging ligand in the active site of the recently reported high-resolution X-ray crystal structures of Cd^{2+}/Cd^{2+}−PTE and Zn^{2+}/Cd^{2+}−PTE should be a hydroxide ion, rather than a water molecule. The protonated active site structures of the Cd^{2+}-containing enzymes are all significantly different from that of Zn^{2+}/Zn^{2+}−PTE. In Cd^{2+}/Cd^{2+}−PTE and Zn^{2+}/Cd^{2+}−PTE, the second bridging ligand always simultaneously coordinates to the two metal ions, whether it is a hydroxide ion or a water molecule. The pK_a values calculated for the second bridging ligand are in good agreement with the observed kinetic pK_a values for both the Cd^{2+}- and Zn^{2+}-substituted enzymes. The calculated results strongly support the conclusion that the observed kinetic pK_a is actually the pK_a of the second bridging ligand, and strongly support the previously postulated catalytic mechanism of PTE involving a bridging hydroxide that attacks the phosphorus center of the substrate.

Introduction

Phosphotriesterase (PTE) from *Pseudomonas diminuta* catalyzes the hydrolysis of a wide variety of organophosphorus pesticides and related nerve agents, i.e., acetylcholinesterase inhibitors, with rate enhancements that approach the diffusion-controlled limit.[1] There is much current interest both in chemistry and biochemistry in understanding how this remarkable enzyme catalyzes the hydrolysis so effectively.[2] It has been known that two divalent metal ions are critical for maximal catalytic activity of the enzyme.[1] The native divalent cations are Zn^{2+}. The two native Zn^{2+} ions can be substituted with either Cd^{2+}, Co^{2+}, Ni^{2+}, or Mn^{2+} with the restoration of full catalytic activity.[3] To elucidate the catalytic mechanism, it is first necessary to determine the structure of the active site. Recently reported extensive experimental studies have provided valuable insights into the structural details concerning the PTE active site.[4−14] ESR spectra of the Mn^{2+}-substituted PTE have indicated that the two metal ions are closely bound and are antiferromagnetically coupled through a common ligand.[5] ^{113}Cd NMR spectroscopic studies have demonstrated that the two enzyme-bound Cd^{2+} ions are in slightly different chemical environments, and that the first coordination shell for each metal is composed of a mixture of oxygen and nitrogen ligands with the exclusion of any thiolate from cysteine residues.[6] The relative importance of histidine residues in metal ligation was examined by site-specific mutation of all seven histidine residues in the protein.[7] The mutagenesis investigations predicted that six of the seven histidine residues were at or near the active site and contributed to the structure and/or catalytic function of the enzyme. This prediction was further confirmed with subsequent X-ray crystallographic analyses of the three-dimensional structure of the apoenzyme.[8]

Furthermore, Benning et al.[9] reported a three-dimensional X-ray crystal structure of Cd^{2+}-substituted PTE, and Vanhooke et al.[10] reported a three-dimensional X-ray crystal structure of Zn^{2+}-substituted PTE complexed with the inhibitor, diethyl 4-methylbenzylphosphonate. These investigators also reported high-resolution X-ray structures of different metal-substituted forms of PTE, including the PTE form with mixed Zn^{2+} and Cd^{2+} ions in the active site.[11,12] Each of these X-ray crystal structures has two bridging ligands to the metals. The first bridging ligand is a carbamylated lysine residue (Lys 169). The second bridging ligand should be either a hydroxide ion or a water molecule, although hydrogen atoms cannot be determined by X-ray diffraction techniques. The more buried Zn^{2+} and Cd^{2+} are all surrounded by His 55, His 57, Lys 169, Asp 301, and the bridging hydroxide/water in a trigonal bipyramidal arrangement. However, the coordination numbers (n) of the second Cd^{2+} and second Zn^{2+} are slightly different. The second Zn^{2+} was either four-coordinated[10] or five-coordinated,[12] whereas the second Cd^{2+} was six-coordinated,[9,12] by Lys 169, His 201, His 230, the bridging hydroxide/water, and $n - 4$ additional water molecules. The X-ray crystal structures also indicated that the two Zn^{2+} ions in the active site are separated by ∼3.3 Å (when four-coordinated)[9] or ∼3.5 Å (when five-coordinated),[12] whereas the two Cd^{2+} ions in the active site are separated by ∼3.7 Å.[12]

The identity of the second bridging ligand in the active site of the X-ray crystal structure of Zn^{2+}-substituted PTE was theoretically determined by performing both molecular dynamics (MD) simulations on the solvated enzyme−inhibitor complex and quantum chemical calculations on simplified models of the active site.[13] The results obtained from both the MD simulations and the quantum chemical calculations consistently indicate that

* Corresponding author. (Currently visiting at Pacific Northwest National Laboratory.) E-mail: Chang-Guo.Zhan@pnl.gov.
[†] Pacific Northwest National Laboratory.
[‡] Columbia University.

10.1021/jp013064k CCC: $22.00
Published on Web 12/15/2001

as the possible second bridging ligands, the hydroxide coordinates to the two zinc ions simultaneously, while the water coordinates only to one zinc. All the results strongly support the conclusion that the second bridging ligand in the active site of the reported X-ray crystal structure of Zn^{2+}-substituted PTE is a hydroxide ion rather than a water molecule. The geometric parameters determined by the quantum chemical calculations, on the system with hydroxide as the second bridging ligand, are all in excellent agreement with the corresponding parameters in the reported X-ray crystal structure of Zn^{2+}-substituted PTE.

It is interesting to know whether the second bridging ligand in the active site of the reported X-ray crystal structures of Cd^{2+}-containing PTE is also a hydroxide ion or not. Kafafi and Krauss recently reported a relevant computational study on metal substitution in PTE active site structure.[15] They examined the active site structures of PTE with two Zn^{2+} ions, with two Cd^{2+} ions, and with one Zn^{2+} and one Cd^{2+}. The enzyme with one Zn^{2+} and one Cd^{2+} is denoted by $Zn^{2+}/Cd^{2+}-$PTE (if the more buried metal ion is Zn^{2+}) or $Cd^{2+}/Zn^{2+}-$PTE (if the more buried metal ion is Cd^{2+}). Their calculations resulted in a prediction[15] that $Cd^{2+}/Zn^{2+}-$PTE is more stable than $Zn^{2+}/Cd^{2+}-$PTE, whereas the latest X-ray structural analysis[12] clearly shows that the X-ray crystal structure is actually $Zn^{2+}/Cd^{2+}-$PTE. Besides, they did not examine the identity of the second bridging ligand. All their calculations[15] were performed on the PTE active site structures in which the second bridging ligand is a hydroxide ion. The possibility of a water molecule acting as the second bridging ligand has not been considered yet.

We therefore attempt to determine the identity of the second bridging ligand in the X-ray crystal structures of Cd^{2+}-substituted PTE (denoted by $Cd^{2+}/Cd^{2+}-$PTE) and $Zn^{2+}/Cd^{2+}-$PTE by performing quantum chemical calculations on two kinds of active site models: one with a water as the second bridging ligand (model **1**) and the other with a hydroxide (model **2**). Comparison of the calculated results with available experimental data provides useful insights into the active site structures and catalytic mechanism.

Calculation Methods

The two kinds of active site models **1** and **2** examined in this study are all based on the reported X-ray crystal structures of $Cd^{2+}/Cd^{2+}-$PTE[9,12] with following simplifications: the carbamylated lysine and aspartic acid functional group are replaced by $NH_2CO_2^-$ and CHO_2^-, respectively; and the His 55, His 57, His 201, and His 230 residues are all simplified as NH_3 molecules. The same simplifications were used in previous quantum chemical calculations on the active site models of Zn^{2+}-substituted PTE.[13] The results calculated for the active site models of Zn^{2+}-substituted PTE indicate that these simplified models are adequate for our purpose of studying the active site structures. All the optimized geometric parameters involving the Zn^{2+} ions are not significantly different from the corresponding parameters optimized for the larger model where each NH_3 is replaced by imidazole.[13] To further examine whether the simplified models are sufficient for qualitatively studying the active site structures of Cd^{2+}-containing PTE or not, we also performed geometry optimization on an active site model for $Cd^{2+}/Cd^{2+}-$PTE, **1L** in which the second bridging ligand is considered as a water molecule, whose size is as large as the PTE models used by Kafafi and Krauss[15] with a hydroxide ion as the second bridging ligand. In model **1L**, each of the four NH_3 molecules in model **1** is replaced by imidazole, and the ligands $NH_2CO_2^-$ and CHO_2^- in model **1** become $CH_3NHCO_2^-$ and $CH_3CO_2^-$, respectively.

The geometries of the active site models **1** and **2** of Cd^{2+}-containing PTE were fully optimized by employing density functional theory (DFT) using Becke's three parameter hybrid exchange functional and the Lee−Yang−Parr correlation functional (B3LYP).[16] The basis set used in the DFT calculations is the 6-31G* for all atoms except for cadmium. An equivalent level of basis set, the DZVP (DFT orbital),[17] was used for cadmium since there is no 6-31G* basis set available for this element. The corresponding vibrational frequencies were evaluated with the optimized geometries to verify their true stability and to evaluate the zero-point vibration energies (ZPVE). Some single-point energy calculations were also performed using the B3LYP-optimized geometries with the same basis set. Previous ab initio and DFT calculations[13] on the active site models of Zn^{2+}-substituted PTE indicate that the geometries of the active site models optimized at the HF/3-21G, HF/6-31G*, B3LYP/6-31G*, and MP2/6-31G* levels of theory for the same model are all consistent with each other. The geometric parameters optimized at the B3LYP/6-31G* level are all very close to the corresponding parameters in the reported X-ray crystal structure and to those optimized at the MP2/6-31G*, HF/6-31G*, and HF/3-21G levels. For further comparison, additional geometry optimizations and corresponding vibrational frequency calculations were performed on models **1L** and **1** at the HF/3-21G level.

Besides, the geometries optimized with the B3LYP calculations for the two active site models **1** and **2** were employed to perform self-consistent reaction field (SCRF) calculations at the Hartree−Fock (HF) level of theory with the same basis set, i.e. the DZVP for cadmium and the 6-31G* for the other atoms, to determine free energies of solvation in aqueous solution. Finally, some additional B3LYP energy calculations with larger basis sets, i.e., the 6-31+G*, 6-311+G**, and 6-311++G** basis sets, for all nonmetal atoms were also carried out in the gas phase to examine the basis set dependence of the energy calculations. The calculated free energy in solution was taken as the gas-phase energy determined by the B3LYP calculation (including ZPVE correction) plus the solvent shift determined by the SCRF calculation at the HF level. The SCRF method employed was developed and implemented recently in the GAMESS program[18] by one of us,[19a] and is called the surface and volume polarizations for electrostatics (SVPE). This procedure is also known as the fully polarizable continuum model (FPCM)[13,20] because both surface and volume polarization effects are fully determined in the SVPE calculation.[19] Since the solute cavity surface is defined as a solute electron charge isodensity contour determined self-consistently during the SVPE iteration process, the SVPE results, converged to the exact solution of Poisson's equation with a given numerical tolerance, depend only on the contour value at a given dielectric constant and a certain quantum chemical calculation level.[19] This single parameter value has been determined as 0.001 au based on an extensive calibration study.[19b]

Unless indicated otherwise, the Gaussian94[21] and Gaussian98[22] programs were used to obtain the present results. All the calculations in this work were performed on Silicon Graphics, Inc., Origin 200 multiprocessor computers.

Results and Discussion

Geometries. Depicted in Figure 1 are the geometries of models **1** and **2** determined for $Cd^{2+}/Cd^{2+}-$PTE by the B3LYP geometry optimizations in which the initial geometries used are all based on the X-ray crystal structures.[9,12] As far as the two Cd atoms and other atoms coordinated to the Cd atoms are

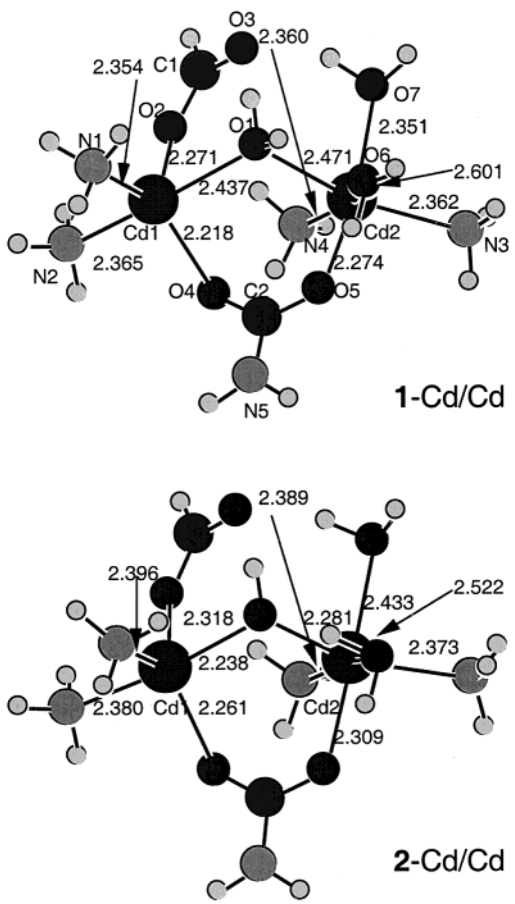

Figure 1. Geometries of models **1**−**Cd/Cd** and **2**−**Cd/Cd** optimized using the B3LYP functional with the DZVP basis set for Cd and the 6-31G* for the other atoms.

concerned, the root-mean-square deviation (RMSD) of the optimized geometry from the X-ray crystal structure[12] of Cd^{2+}/Cd^{2+}−PTE is ∼0.8 Å for both **1** and **2**. The RMSD value of ∼0.8 Å is smaller than the resolution of 1.3 Å for the X-ray crystal structure[12] and smaller than the RMSD value of ∼1.0 Å in our previous molecular dynamics simulations[13,14] on solvated PTE structures at room temperature. This implies that the overall agreement between the X-ray crystal structure and the optimized geometries is good and that the effects of protein environment on the geometric parameters within the active site should not be dramatic. The important internuclear distances optimized are summarized in Table 1 compared with the experimental data from the latest high-resolution X-ray crystal structure.[12] We also tested a geometry optimization for model **2** starting from the optimized geometry of model **1** by removing a proton from the bridging water, and a geometry optimization for model **1** starting from the optimized geometry of model **2** by adding a proton to the bridging hydroxide. It turned out that the geometry optimizations starting from different initial geometries eventually lead to the same results.

It is interesting to compare the geometries optimized for the active site models of Cd^{2+}/Cd^{2+}−PTE with those for the corresponding active site models Zn^{2+}/Zn^{2+}−PTE.[13] First of all, we focus on the PTE active site structures in which the second bridging ligand is considered as a water molecule. In model **1** of Cd^{2+}/Cd^{2+}−PTE, the bridging water oxygen simultaneously coordinates to the two cadmium, whereas the water oxygen in the corresponding model of Zn^{2+}/Zn^{2+}−PTE coordinates only to one zinc.[13] To further theoretically confirm this remarkable difference, we tried to re-optimize the geometry

TABLE 1: Optimized Internuclear Distances (in Å) Compared with Those in the X-ray Crystal Structures of Phosphotriesterases

	M1/M2 = Cd/Cd						M1/M2 = Zn/Cd		
	HF[b]		B3LYP[c]				B3LYP[c]		
distance	**1L**	**1**	**1**	**2**	**2a**	X-ray[a]	**1**	**2**	X-ray[a]
M1-O1	2.386	2.359	2.437	2.238	2.247	2.2	2.411	2.000	2.0
M1-O2	2.272	2.241	2.271	2.318	2.296	2.3	1.985	2.096	2.1
M1-O4	2.213	2.173	2.218	2.261	2.323	2.2	1.939	1.994	2.3
M1-N1	2.320	2.346	2.354	2.396	2.388	2.1	2.071	2.148	2.0
M1-N2	2.305	2.356	2.365	2.380	2.374	2.2	2.108	2.154	2.1
M2-O1	2.378	2.489	2.471	2.281	2.218	2.2	2.358	2.278	2.1
M2-O5	2.266	2.259	2.274	2.309	2.268	2.3	2.273	2.271	2.2
M2-N3	2.310	2.366	2.362	2.373	2.336	2.2	2.319	2.382	2.2
M2-N4	2.386	2.373	2.360	2.389	2.355	2.3	2.315	2.390	2.2
M1-M2	3.670	3.940	3.976	3.558	3.591	3.7	3.718	3.405	3.6
M2-O6	2.338	3.386	2.601	2.522	2.552	2.5	3.213	2.523	2.8
M2-O7	2.286	2.259	2.351	2.433	3.627	2.0	2.401	2.390	2.5

[a] X-ray crystal structure from ref 9. [b] The HF geometry optimizations with the 3-21G basis set. [c] The B3LYP geometry optimizations with the DZVP basis set for Cd and the 6-31G* for the other atoms.

of the active site model of Zn^{2+}/Zn^{2+}−PTE with a water molecule as the second bridging ligand starting from the coordinates of the optimized geometry of model **1** of Cd^{2+}/Cd^{2+}−PTE, but replacing the two cadmium with two zinc. The output indicated that the internuclear distance between the first zinc (Zn1 corresponding to Cd1 in Figure 1) and the bridging water oxygen became longer and longer during the optimization process. We stopped the optimization after the distance became longer than 3.5 Å. Due to this remarkable difference, the change of the optimized cadmium−cadmium internuclear distance caused by the replacement of the bridging hydroxide with water is significantly different from the corresponding change of the zinc−zinc distance. Changing the second bridging ligand from hydroxide (model **1**) to water (model **2**), the optimized cadmium−cadmium distance becomes only ∼0.4 Å longer for Cd^{2+}/Cd^{2+}−PTE, whereas the optimized zinc−zinc distance becomes ∼1 Å longer for Zn^{2+}/Zn^{2+}−PTE.[13] In addition, the bond lengths between the zinc and coordinated ligands in Zn^{2+}/Zn^{2+}−PTE[13] are systematically shorter than the corresponding bond lengths between the cadmium and ligands in Cd^{2+}/Cd^{2+}−PTE by about 0.2−0.3 Å. This systematic increase of the bond lengths is consistent with the increase of the ionic radius from Zn^{2+} (0.74 Å) to Cd^{2+} (0.97 Å).[23]

Concerning reliability of the conclusion about the bridging water molecule, as seen in Table 1 the geometry of model **1** optimized at the HF/3-21G level is consistent with that determined by the B3LYP geometry optimization. The geometry of a larger active site model **1L** (depicted in Figure 2) optimized at the HF/3-21G level is qualitatively consistent with that of small model **1** optimized at the same level, thus illustrating that the small model used is indeed sufficient for qualitatively examining the PTE active site structure.

When the second bridging ligand is considered as a hydroxide ion, the hydroxide oxygen coordinates to the two metal ions simultaneously for both the Zn^{2+}- and Cd^{2+}-substituted enzymes. For the most stable geometry of Cd^{2+}/Cd^{2+}−PTE model, i.e., model **2**, the second cadmium is six-coordinated as shown in Figure 1. We also found another local minimum on the potential energy surface associated with model **2a** (depicted in Figure 2) in which the second cadmium is five-coordinated; only one water molecule coordinates to the cadmium and the other water molecule extremely strongly hydrogen-bonds to the bridging hydroxide. The calculated Gibbs free energy of model **2a** is only ∼0.6 kcal/mol higher than that of model **2**. The

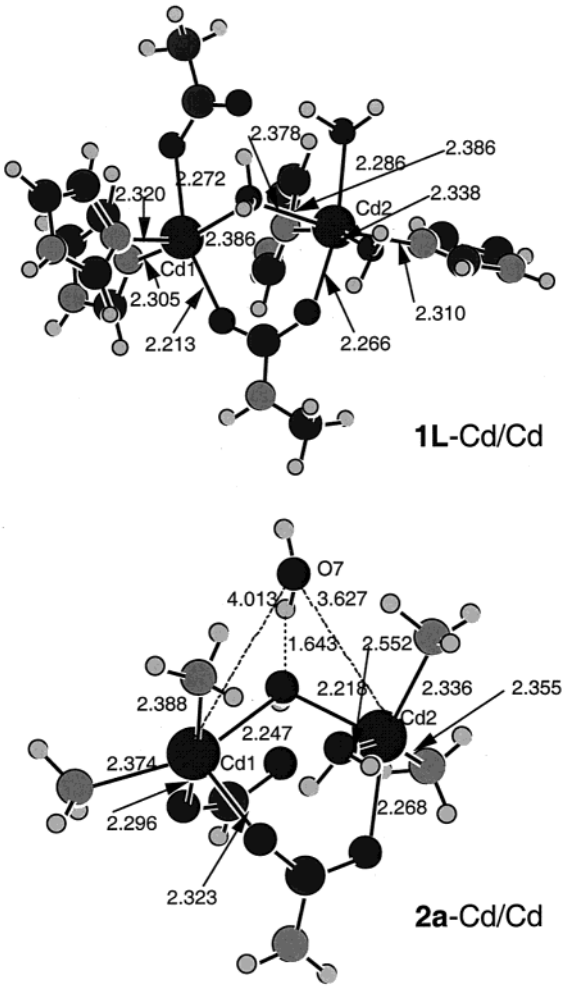

Figure 2. Geometry of model **1L**−**Cd/Cd** optimized at the HF/3-21G level and geometry of model **2a**−**Cd/Cd** optimized using the B3LYP functional with the DZVP basis set for Cd and the 6-31G* for the other atoms.

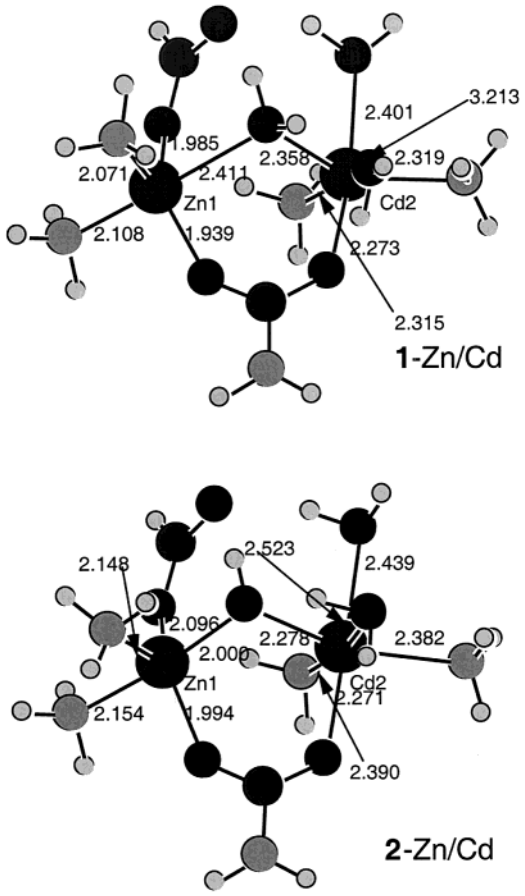

Figure 3. Geometries of models **1**−**Zn/Cd** and **2**−**Zn/Cd** optimized using the B3LYP functional with the DZVP basis set for Cd and the 6-31G* for the other atoms.

optimized cadmium−cadmium internuclear distance, ∼3.6 Å, in model **2** (and **2a**) is slightly longer than corresponding zinc−zinc distance, ∼3.3 or 3.5 Å.[13]

Comparing the optimized geometries of Cd^{2+}/Cd^{2+}−PTE with the X-ray crystal structures, both models **1** and **2** are qualitatively consistent with the latest X-ray crystal structure of Cd^{2+}/Cd^{2+}−PTE.[12] The optimized geometric parameters of model **2** are closer to the corresponding experimental values,[12] particularly for the internuclear distances between the bridging hydroxide/water oxygen and the two cadmium ions. It is likely that the second bridging ligand in the latest X-ray crystal structure of Cd^{2+}/Cd^{2+}−PTE[12] is a hydroxide ion, rather than a water molecule. The earlier X-ray crystal structure of Cd^{2+}/Cd^{2+}−PTE, in which the internuclear distances between hydroxide/water oxygen and the two Cd^{2+} ions are all ∼2.7 Å, with a lower resolution[9] could be a mixture of two possible Cd^{2+}/Cd^{2+}−PTE structures corresponding to models **2** and **2a**.[24]

We also examined the Zn^{2+}/Cd^{2+}−PTE active site structures using the same computational protocol used for Cd^{2+}/Cd^{2+}−PTE. The initial geometries used in the geometry optimizations for Zn^{2+}/Cd^{2+}−PTE are the optimized geometries of models **1** and **2** for Cd^{2+}/Cd^{2+}−PTE but the first cadmium is replaced by zinc. Now that a water molecule can bridge the two Cd^{2+} ions in Cd^{2+}/Cd^{2+}−PTE but cannot bridge the two Zn^{2+} ions in Zn^{2+}/Zn^{2+}−PTE, it is interesting to know whether a water molecule can bridge a Zn^{2+} and a Cd^{2+} in Zn^{2+}/Cd^{2+}−PTE or not. As depicted in Figure 3, the optimized geometry of model **1** for Zn^{2+}/Cd^{2+}−PTE (denoted by **1**−Zn/Cd) is similar to model **1** for Cd^{2+}/Cd^{2+}−PTE. The only difference is the systematic shortening of the bond lengths involving the first metal ion due to the change of the ionic radius. So, a water molecule can also bridge the two mixed metal ions in Zn^{2+}/Cd^{2+}−PTE. Further, the optimized geometry of model **2** for Zn^{2+}/Cd^{2+}−PTE (denoted by **2**−Zn/Cd) is also similar to model **2** for Cd^{2+}/Cd^{2+}−PTE. The second cadmium ion in **2**−Zn/Cd is also six-coordinated. We also tested a geometry optimization for a possible Cd^{2+}/Zn^{2+}−PTE structure starting from the optimized geometry of model **2** for Cd^{2+}/Cd^{2+}−PTE but the second cadmium is replaced by zinc. In the optimized geometry of model **2** for Cd^{2+}/Zn^{2+}−PTE (not shown), the second metal ion (i.e., Zn^{2+}) is four-coordinated; during the optimization process the two water molecules left the zinc ion and hydrogen-bond to other ligands. So the reported high-resolution X-ray crystal structure[12] of PTE with one Zn^{2+} and one Cd^{2+} is not consistent with the hypothetical Cd^{2+}/Zn^{2+}−PTE structure; it is only consistent with the Zn^{2+}/Cd^{2+}−PTE structure. The second bridging ligand in Zn^{2+}/Cd^{2+}−PTE active site is also likely a hydroxide ion because the optimized geometric parameters with a hydroxide as the second bridging ligand are closer to those in the X-ray crystal structure,[12] particularly for the distances between the bridging hydroxide/water oxygen and the metal ions.

We note that our conclusion regarding Zn^{2+}/Cd^{2+}−PTE vs Cd^{2+}/Zn^{2+}−PTE is contrary to that obtained by Kafafi and Krauss[15] in their calculations. Their conclusion was based on the calculated relative energies of Zn^{2+}/Cd^{2+}− and Cd^{2+}/Zn^{2+}−

TABLE 2: The pK_a Values Calculated for the Second Bridging Ligand in the Active Site of Phosphtriesterases Compared with the Experimental Kinetic pK_a Values

	calc.[a]				
	6-31G*	6-31+G**	6-311+G**	6-311++G**	expt[b]
Cd−PTE	9.7	8.1	8.5	8.4	8.1
Zn−PTE	5.9	5.1	5.2	5.1	5.8

[a] Based on the geometries optimized using the B3LYP functional with the DZVP basis set for Cd and the 6-31G* for the other atoms. All the pK_a values were calculated with $T = 298$ K. See text for the details of the pK_a calculations. The basis sets indicated here refer to those used for nonmetal atoms in the gas-phase B3LYP energy calculations. [b] Kinetic pK_a values from ref 3.

PTE structures; their calculated energy of Cd^{2+}/Zn^{2+}−PTE structure is lower than that of Zn^{2+}/Cd^{2+}−PTE structure. However, as recognized recently by Benning et al.,[12] their calculations[15] apparently neglected the tendency of the more solvent-exposed M2 site to expand its inner-sphere ligands with added water molecules, because they did not consider coordination of water molecules so that the coordination number for the second metal ion (M2) is always 4 no matter whether it is Zn^{2+} or Cd^{2+}. Further accounting for the effects of the two additional water molecules, the Gibbs free energy of Zn^{2+}/Cd^{2+}−PTE structure (model **1**) calculated using the MP2 method with the B3LYP-optimized geometry (including the thermal corrections determined by the B3LYP calculation) is about 2 kcal/mol lower than the corresponding free energy of Cd^{2+}/Zn^{2+}−PTE structure. Our calculated results are all in good agreement with the latest X-ray crystal structure.[12]

pK_a. To theoretically evaluate the pK_a value of the second bridging ligand of Cd^{2+}-substituted PTE, we consider the free energy change ΔG_a for the model reaction

$$\mathbf{1}\ (\text{solvated}) \rightarrow \mathbf{2}\ (\text{solvated}) + H^+\ (\text{solvated}) \qquad (1)$$

The ΔG_a is determined by using the free energies calculated for models **1** and **2** and the experimental data for a proton as used by Lim et al.[25] The pK_a value is evaluated by the ΔG_a value through

$$pK_a = \Delta G_a/(2.303RT) \qquad (2)$$

The same theoretical procedure was also performed for the Zn^{2+}-substituted PTE.[13] The calculated pK_a values of the second bridging ligand are summarized in Table 2. One can see from Table 2 that the calculated pK_a values become slightly smaller when the 6-31G* basis set, used for nonmetal atoms, is replaced by 6-31+G**. However, further increasing the basis functions from the 6-31+G** to 6-311+G** and 6-311++G** does not considerably change the calculated pK_a values. We therefore assume that the 6-311++G** basis set is adequate for the pK_a evaluation. The pK_a value of 8.4 calculated for Cd^{2+}-substituted PTE indicates that when the pH value is about 8.4, the concentrations of the two structural forms of Cd^{2+}-substituted PTE (with hydroxide and with water as the second bridging ligand) should be equal to each other. As comparison, the pK_a value for the Zn^{2+}/Cd^{2+}−PTE was calculated as 6.4 using the 6-311++G** basis set. The pK_a value of 6.4 calculated for Zn^{2+}/Cd^{2+}−PTE is between the pK_a values for Zn^{2+}/Zn^{2+}−PTE and Cd^{2+}/Cd^{2+}−PTE, and is closer to the pK_a value of 5.1 for Zn^{2+}/Zn^{2+}−PTE.

It should be pointed out that these pK_a values were evaluated using simplified active site models without specific consideration of the more complicated protein environment. Comparing the chemical environment of the second bridging ligand in models **1** and **2** with the corresponding protein environment, one can see that the primary difference exists in the nonbonded interactions across three bonds between the bridging hydroxide/water oxygen and other protein atoms and in other nonbonded interactions. Further, we used the same level of structural simplifications for all the substituted enzymes. Thus, it is not surprising that the relative magnitudes of the pK_a values associated with the second bridging ligand for these enzymes are well reproduced by our calculations based on models **1** and **2**.

It is interesting to compare the pK_a calculated for the second bridging ligand with the kinetic pK_a of PTE determined through the experimental pH−rate profile. With the pH−rate profile for Zn^{2+}-substituted PTE, it was demonstrated that the kinetic pK_a is associated with a functional group, and that this group was most likely a histidine residue that acts as a general base in the abstraction of a proton from an activated water molecule.[26] A more detailed kinetic pK_a study[3] indicated that the kinetic pK_a depends on the exact metal composition. The observed kinetic pK_a values are lowest with zinc (5.8) and highest with cadmium (8.1).[3] These results are consistent with the direct coordination of the hydrolytic water molecule (or hydroxide ion) with one or both of the metal ions in the active site. The metal ion was then believed to modulate the pK_a of the active site histidine.[3] The X-ray crystal structures of the Cd^{2+}- and Zn^{2+}-substituted enzymes[9,10−12] show a solvent water molecule (or hydroxide ion) bridging the two metal ions. However, an obvious general base has not been identified. So, it seems reasonable to consider that the observed kinetic pK_a is associated with the second bridging ligand in the PTE active site.[2a] Interestingly, as seen in Table 2, the pK_a values calculated for the second bridging ligand are in good agreement with the observed kinetic pK_a values for both the Cd^{2+}- and Zn^{2+}-substituted enzymes. Thus, the calculated results together with the X-ray crystal structures[9,10−12] strongly support the conclusion that the observed kinetic pK_a is the pK_a of the second bridging ligand. Therefore, the rate of the PTE-catalyzed hydrolysis of the substrate depends on the concentration of the structural form with hydroxide as the second bridging ligand. When the pH of the aqueous solution of PTE is equal to the kinetic pK_a value, the concentration of the PTE structure with hydroxide as the second bridging ligand should be equal to that with water molecule as the second bridging ligand. At lower pH the structural form with water as the second bridging ligand should be dominant, and at higher pH the structural form with hydroxide as the second bridging ligand should be dominant. So the concentration of the PTE active site structure with the bridging hydroxide is a function of the pH, which is qualitatively consistent with the observed pH−rate profile[3,26] and strongly support the postulated catalytic mechanism of PTE for the bridging hydroxide attacking the phosphorus center of the substrate proposed by Vanhooke et al.[10]

Conclusion

The calculated results indicate that the second bridging ligand in the active site of the recently reported high-resolution X-ray crystal structures of two Cd^{2+}-containing phosphotriesterases (PTE), i.e., Cd^{2+}/Cd^{2+}−PTE and Zn^{2+}/Cd^{2+}−PTE, should be a hydroxide ion, rather than a water molecule. While the coordination of the bridging hydroxide ion in the active site of Cd^{2+}-containing PTE is similar to that in Zn^{2+}/Zn^{2+}−PTE, the protonated active site structures of Cd^{2+}-containing PTEs are all significantly different from that of Zn^{2+}/Zn^{2+}−PTE. For Zn^{2+}/Zn^{2+}−PTE, when the second bridging ligand is a hydroxide the hydroxide oxygen coordinates to the two zinc ions

simultaneously, while when the second bridging ligand is a water molecule the water oxygen coordinates only to one zinc. However, for both Cd^{2+}/Cd^{2+}−PTE and Zn^{2+}/Cd^{2+}−PTE the second bridging ligand always simultaneously coordinates to the two metal ions whether it is a hydroxide ion or a water molecule. The remarkable difference is associated with the coordination of the bridging water molecule. Due to the difference, the change of the cadmium−cadmium internuclear distance caused by the replacement of the bridging hydroxide with water is significantly different from the corresponding change of the zinc−zinc distance. Changing the second bridging ligand from hydroxide to water, the optimized zinc−zinc distance becomes ∼1 Å longer for Zn^{2+}/Zn^{2+}−PTE, whereas the optimized cadmium−cadmium distance becomes only ∼0.4 Å longer for Cd^{2+}/Cd^{2+}−PTE and the optimized zinc−cadmium distance becomes only ∼0.3 Å longer for Zn^{2+}/Cd^{2+}−PTE. However, ignoring the water molecules in the active site, the optimized bond lengths between the cadmium ions and other ligands are just systematically longer than the corresponding optimized bond lengths between the zinc and ligands by about 0.2−0.3 Å. This systematic increase of the bond lengths is consistent with the increase of the ionic radius from Zn^{2+} (0.74 Å) to Cd^{2+} (0.97 Å).

The pK_a values calculated for the second bridging ligand are in good agreement with the observed kinetic pK_a values for both the Cd^{2+}- and Zn^{2+}-substituted enzymes. The calculated results strongly support the conclusion that the observed kinetic pK_a is actually the pK_a of the second bridging ligand, and strongly support the postulated catalytic mechanism of PTE for the bridging hydroxide attacking the phosphorus center of the substrate proposed by Vanhook et al.[10]

Acknowledgment. This work was supported partially by the Laboratory Directed Research and Development Program (LDRD) at Pacific Northwest National Laboratory. Pacific Northwest National Laboratory is a multiprogram national laboratory operated for the U.S. Department of Energy by Battelle Memorial Institute under contract DE-AC06-76RLO 1830. F.Z. worked at PNNL with a Faculty Fellowship administrated by Associated Western Universities, Inc.

References and Notes

(1) Dumas, D. P.; Caldwell, S. R.; Wild, J. R.; Raushel, F. M. *J. Biol. Chem.* **1989**, *264*, 19659.

(2) (a) Hong, S.-B.; Raushel, F. M. *Biochemistry* **1996**, *35*, 10904. (b) Kuo, J. M.; Chae, M. Y.; Raushel, F. M. *Biochemistry* **1997**, *36*, 1982. (c) Hong, S.-B.; Mullins, L. S.; Shim, H.; Raushel, F. M. *Biochemistry* **1997**, *36*, 9022. (d) Seo, J. S.; Hynes, R. C.; Williams, D.; Chin, J. *J. Am. Chem. Soc.* **1998**, *120*, 9945. (e) Hong, S.-B.; Raushel, F. M. *Biochemistry* **1999**, *38*, 1159.

(3) Omburo, G. A.; Kuo, J. M.; Mullins, L. S.; Raushel, F. M. *J. Biol. Chem.* **1992**, *267*, 13278.

(4) Lewis, V. E.; Donarski, W. J.; Wild, J. R.; Raushel, F. M. *Biochemistry* **1988**, *27*, 1591.

(5) Chae, M. Y.; Omburo, G. A.; Kuo, J. M.; Lindahl, P. A.; Raushel, F. M. *J. Am. Chem. Soc.* **1993**, *115*, 12173.

(6) Omburo, G. A.; Mullins, L. S.; Raushel, F. M. *Biochemistry* **1993**, *32*, 9148.

(7) (a) Kuo, J. M.; Raushel, F. M. *Biochemistry* **1994**, *33*, 4265. (b) Lai, K.; Dave, K. I.; Wild, J. R. *J. Biol. Chem.* **1994**, *269*, 16579. (c) Banzon, J. A.; Kuo, J. M.; Miles, B. W.; Fischer, D. R.; Stang, P. J.; Raushel, F. M. *Biochemistry* **1995**, *34*, 743. (d) Banzon, J. A.; Kuo, J. M.; Fischer, D. R.; Stang, P. J.; Raushel, F. M. *Biochemistry* **1995**, *34*, 750.

(8) Benning, M. M.; Kuo, J. M.; Raushel, F. M.; Holden, H. M. *Biochemistry* **1994**, *33*, 15001.

(9) Benning, M. M.; Kuo, J. M.; Raushel, F. M.; Holden, H. M. *Biochemistry* **1995**, *34*, 7973.

(10) Vanhooke, J. L.; Benning, M. M.; Raushel, F. M.; Holden, H. M. *Biochemistry* **1996**, *35*, 6020.

(11) Benning, M. M.; Hong, S.-B.; Raushel, F. M.; Holden, H. M. *J. Biol. Chem.* **2000**, *275*, 30556.

(12) Benning, M. M.; Shim, H.; Raushel, F. M.; Holden, H. M. *Biochemistry* **2001**, *40*, 2712.

(13) Zhan, C.-G.; Norberto de Souza, O.; Rittenhouse, R.; Ornstein, R. L. *J. Am. Chem. Soc.* **1999**, *121*, 7279.

(14) Koca, J.; Zhan, C.-G.; Rittenhouse, R.; Ornstein, R. L. *J. Am. Chem. Soc.* **2001**, *123*, 817.

(15) Kafafi, S. A.; Krauss, M. *Int. J. Quantum Chem.* **1999**, *75*, 289.

(16) (a) Becke, A. D. *J. Chem. Phys.* **1993**, *98*, 5648. (b) Lee, C.; Yang, W.; Parr, R. G. *Phys. Rev. B* **1988**, *37*, 785.

(17) (a) Godbout, N.; Salahub, D. R.; Andzelm, J.; Wimmer, E. *Can. J. Chem.* **1992**, *70*, 560. (b) Basis sets were obtained from the Extensible Computational Chemistry Environment Basis Set Database, Version 1999, as developed and distributed by the Molecular Science Computing Facility, Environmental and Molecular Sciences Laboratory, which is part of the Pacific Northwest Laboratory, P.O. Box 999, Richland, WA 99352, and funded by the U.S. Department of Energy. The Pacific Northwest Laboratory is a multi-program laboratory operated by Battelle Memorial Institue for the U.S. Department of Energy under contract DE-AC06-76RLO 1830. Contact David Feller or Karen Schuchardt for further information.

(18) Schmidt, M. W.; Baldridge, K. K.; Boatz, J. A.; Elbert, S. T.; Gordon, M. S.; Jensen, J. H.; Koseki, S.; Matsunaga, N.; Nguyen, K. A.; Su, S. J.; Windus, T. L.; Dupuis, M.; Montgomery, J. A. *J. Comput. Chem.* **1993**, *14*, 1347.

(19) (a) Zhan, C.-G.; Bentley, J.; Chipman, D. M. *J. Chem. Phys.* **1998**, *108*, 177. (b) Zhan, C.-G.; Chipman, D. M. *J. Chem. Phys.* **1998**, *109*, 10543. (c) Zhan, C.-G.; Chipman, D. M. *J. Chem. Phys.* **1999**, *110*, 1611.

(20) (a) Zhan, C.-G.; Landry, D. W.; Ornstein, R. L. *J. Am. Chem. Soc.* **2000**, *122*, 2621. (b) Zhan, C.-G.; Zheng, F. *J. Am. Chem. Soc.* **2001**, *123*, 2835. (c) Zhan, C.-G.; Niu, S.; Ornstein, R. L. *J. Chem. Soc., Perkin Trans. 2* **2001**, *1*, 23. (d) Zhan, C.-G.; Landry, D. W. *J. Phys. Chem. A* **2001**, *105*, 1296.

(21) Frisch, M. J.; Trucks, G. W.; Schlegel, H. B.; Gill, P. M. W.; Johnson, B. G.; Robb, M. A.; Cheeseman, J. R.; Keith, T.; Petersson, G. A.; Montgomery, J. A.; Raghavachari, K.; Al-Laham, M. A.; Zakrzewski, V. G.; Ortiz, J. V.; Foresman, J. B.; Cioslowski, J.; Stefanov, B. B.; Nanayakkara, A.; Challacombe, M.; Peng, C. Y.; Ayala, P. Y.; Chen, W.; Wong, M. W.; Andres, J. L.; Replogle, E. S.; Gomperts, R.; Martin, R. L.; Fox, D. J.; Binkley, J. S.; Defrees, D. J.; Baker, J.; Stewart, J. P.; Head-Gordon, M.; Gonzalez, C.; Pople, J. A. *Gaussian 94*, Revision D.1; Gaussian, Inc., Pittsburgh, PA, 1995.

(22) Frisch, M. J.; Trucks, G. W.; Schlegel, H. B.; Scuseria, G. E.; Robb, M. A.; Cheeseman, J. R.; Zakrzewski, V. G.; Montgomery, J. A.; Stratmann, R. E.; Burant, J. C.; Dapprich, S.; Millam, J. M.; Daniels, A. D.; Kudin, K. N.; Strain, M. C.; Farkas, O.; Tomasi, J.; Barone, V.; Cossi, M.; Cammi, R.; Mennucci, B.; Pomelli, C.; Adamo, C.; Clifford, S.; Ochterski, J.; Petersson, G. A.; Ayala, P. Y.; Cui, Q.; Morokuma, K.; Malick, D. K.; Rabuck, A. D.; Raghavachari, K.; Foresman, J. B.; Cioslowski, J.; Ortiz, J. V.; Stefanov, B. B.; Liu, G.; Liashenko, A.; Piskorz, P.; Komaromi, I.; Gomperts, R.; Martin, R. L.; Fox, D. J.; Keith, T.; Al-Laham, M. A.; Peng, C. Y.; Nanayakkara, A.; Gonzalez, C.; Challacombe, M.; Gill, P. M. W.; Johnson, B.; Chen, W.; Wong, M. W.; Andres, J. L.; Gonzalez, A. C.; Head-Gordon, M.; Replogle, E. S.; Pople, J. A. *Gaussian 98*, Revision A.6; Gaussian, Inc., Pittsburgh, PA, 1998.

(23) *CRC Handbook of Chemistry and Physics*, 76th ed.; Lide, D. R., Ed.; CRC Press: New York, 1996.

(24) This hypothesis is consistent with various observations and principles. First of all, as clearly reported by the authors of ref 9, the coordinations of the two additional water molecules to the second Cd^{2+} ion in the earlier X-ray crystal structure are uncertain. They found a "tube" of electron density attached to the metal-bridging water/hydroxide that was difficult to interpret, and it was tentatively modelled as two additional water molecules coordinating to the second Cd^{2+} ion. Thus, no decisive criterion exists for identifying the second bridging ligand in the reported X-ray crystal structure of Cd^{2+}-substituted PTE. In addition, the calculated free energies of models **2** and **2a** so close that both had chances to exist in the crystal depending on the condition of crystal growth. Assuming that the reported crystal existed in the structural form like model **2a**, the second bridging ligand may be regarded as a hydroxide plus a water molecule which strongly hydrogen-bonds to the hydroxide. When the bridging hydroxide plus a water molecule hydrogen-bonded to the hydroxide is modeled as a simple hydroxide (or water), its position is expected to be an average of the real hydroxide and the real water molecule. According to this assumption, the average distance between the second bridging ligand and the two cadmiun ions in model **2a** should be ∼3.03 Å compared to the corresponding average value, ∼2.26 Å, for model **2**. Further assuming that the reported crystal is close to a simple 1:1 mixture of two structural forms such as models **2** and **2a**, the average distance between the second bridging ligand and the two cadmiun ions should be close to ∼2.65 Å which is in excellent agreement with the experimental value of ∼2.7 Å.

(25) Lim, C.; Bashford, D.; Karplus, M. *J. Phys. Chem.* **1991**, *95*, 5610.

(26) Dumas, D. P.; Raushel, F. M. *J. Biol. Chem.* **1990**, *265*, 21498.